

UDC 548.73:543.422:548.737

**STRUCTURAL STUDY OF THE STABILITY OF THE CAPTOPRIL DRUG REGARDING
THE FORMATION OF ITS CAPTOPRIL DISULPHIDE DIMER**

M.C. de Souza¹, L.F. Diniz¹, C.H. de Jesus Franco¹, H.A. de Abreu², R. Diniz¹

¹*Departamento de Química, ICE / Universidade Federal de Juiz de Fora – Campus Universitário, Brazil*

E-mail: renata.diniz@ufjf.edu.br

²*Departamento de Química, Universidade Federal de Minas Gerais, Belo Horizonte, Brazil*

Received May, 5, 2015

Revised — April, 6, 2016

Captopril disulphide is obtained under hydrothermal conditions. The IR and Raman spectra data are in agreement with the X-ray diffraction results. The disappearance of the band at 2566 cm^{-1} ($\nu(\text{SH})$) in both spectra of captopril disulphide is consistent with the formation of the S—S bond. The degradation of the captopril drug is investigated by Raman spectroscopy and the results indicate that after 6 weeks of air exposure, a band at 512 cm^{-1} , assigned as $\nu(\text{SS})$, is observed, suggesting the formation of captopril disulphide. DFT calculations in the solid state are performed for captopril and captopril disulphide. The results indicate that captopril disulphide is approximately $30\text{ kcal}\cdot\text{mol}^{-1}$ more stable than captopril. The analysis of the total density of states (DOS) reveals that the captopril valence band contains a significant contribution from the S atom, whereas for captopril disulphide, the O atom is the most important for the valence band.

DOI: 10.15372/JSC20160608

Keywords: hypertension, ACE inhibitor, crystal structure, X-ray diffraction.

INTRODUCTION

Hypertension is a major health problem throughout the world due to its high prevalence [1]. Hypertension occurs when blood pressure levels are above the reference values for the general population [2]. Some of the most effective drugs employed in the treatment of arterial hypertension are angiotensin I-converting enzyme (ACE) inhibitors. ACE is a zinc-containing dipeptidyl carboxypeptidase that plays a critical physiological role in blood pressure regulation, converting angiotensin I inactive decapeptide to angiotensin II potent vasopressor octapeptide by removing C-terminal His—Leu dipeptide [3]. The ACE inhibitors have a variety of indications ranging from mild hypertension to post myocardial infarction [4].

Captopril (1-[(2S)-3-mercaptopro-2-methylpropionyl]-L-proline) was the first nonpeptidic orally active ACE inhibitor utilized for the treatment of hypertension. Captopril is an efficient ACE inhibitor via the oral route and is commonly used to treat high blood pressure, congestive heart failure, and cardiovascular disease. It is also employed alone or in combination for the treatment of hypertension [3]. Captopril is considered a drug of choice in antihypertensive therapy because of its effectiveness and low toxicity [5].

Captopril in the solid form has considerable stability. However, it is highly susceptible to oxidation caused by high temperatures, humidity, air exposure or mixture with hygroscopic excipients. The captopril disulphide dimer is an impurity formed in the oxidative process of captopril. The degradation

reaction of captopril forming captopril disulphide has been described in the literature by several authors [6, 7]. All reactions involve the formation of the thiolate anion and subsequent radical mechanism. In addition to a reduction in the active principle by degradation, the presence of a large amount of disulphide reduces the therapeutic adhesion [6].

The mechanism of the action of the captopril ACE inhibitor antihypertensive drug is related to the formation of a (*in vivo*) complex with the catalytic Zn²⁺ ion present at the active site of angiotensin I-converting enzyme. In this complex, the coordination geometry of the Zn²⁺ ion is tetrahedral. The Zn²⁺ centre is coordinated to two histidine molecules by two nitrogen atoms of the imidazole ring, to one acetate ion by one oxygen atom and to the captopril drug molecule by a sulphur atom. The captopril drug interacts with some amino acids by hydrogen bonds that are sufficient to act as a backstop, positioning the substrate molecule [3, 8]. Recently, the captopril complex with a zinc atom was described. In this investigation, it was observed that an *in vitro* reaction causes the formation of a three-dimensional (3D) polymer where Zn²⁺ is coordinated to a S atom, as observed in the crystal structure with the enzyme [8] as well as to carboxylate groups of the drug molecules [9].

This work consisted of experimental and theoretical structural characterizations of captopril disulphide as well as the captopril drug stability in the solid state. A topological analysis of the captopril—zinc coordination polymer was also performed. The molecular details given by these structures can be used to improve the design of new and more potent inhibitors of ACE to combat high blood pressure [10, 11].

EXPERIMENTAL

All chemicals for the syntheses and analyses were of analytical grade and used without further purification. Elemental analyses for C, H, and N were performed on a Perkin-Elmer 2400 analyzer. The infrared spectra were recorded on an Alpha Bruker FT-IR spectrophotometer using KBr pellets in the range of 4000 to 400 cm⁻¹ with an average of 64 scans and 4 cm⁻¹ of spectral resolution. Fourier-transform Raman spectroscopy was performed using a Bruker RFS 100 instrument, a Nd³⁺/YAG laser operating at 1064 nm in the near-infrared and a CCD detector cooled with liquid nitrogen. Good signal-to-noise ratios were obtained by accumulating 256 scans using a spectral resolution of 4 cm⁻¹ and a laser power of 100 mW.

Synthesis and chemical characterisation of captopril disulphide compound (CAPDIS). The captopril disulphide compound was synthesised under hydrothermal conditions. Approximately 8 ml of an aqueous solution containing captopril (0.23 mmol) was added to 8 ml of an aqueous solution containing ZnSO₄·7H₂O (0.11 mmol). This mixture was transferred to a 23-ml Teflon-lined Parr acid digestion bomb. The reaction vessel was heated at 87 °C for 24 h, and after this time, it was slowly cooled to 25 °C. The resulting clear solution was transferred to a beaker and set aside. After 7 days, colourless crystals suitable for the X-ray diffraction analysis formed with a yield of 20 %. The elemental analysis indicated C₁₈H₂₈N₂O₆S₂: calcd. (%): C 49.98, H 6.52, N 6.48; found (%): C 50.03, H 6.55, N 6.43.

Synthesis and chemical characterisation of the Zn²⁺ complex with the captopril drug (CAPZn). An ethanol solution (10 ml) of ZnCl₂ (0.35 mmol) was slowly added to a captopril solution (0.23 mmol) in dimethylformamide (10 ml). The resulting solution was allowed to stand at room temperature. After 1 week, colourless crystals suitable for the X-ray diffraction analysis formed with a yield of 47 %. The elemental analysis indicated C₉H₁₃NO₃SZn: calcd. (%): C 38.52, H 4.67, N 4.99; found (%): C 38.53, H 5.03, N 5.11.

Single crystal X-ray diffraction. Prismatic single crystal X-ray data were collected using an Oxford GEMINI A-Ultra diffractometer with MoK_α radiation ($\lambda = 0.71073 \text{ \AA}$) at room temperature. Data collection, reduction and cell refinement were performed with the Crysaliis program suite [12]. Final unit cell parameters were based on the fitting of all reflection positions. A multiscan absorption correction was applied [13]. The structures were solved and refined using the SHELX-97 program package [14]. Anisotropic displacement parameters were assigned to all non-hydrogen atoms. The H atoms were located in difference Fourier maps and were subsequently geometrically optimized and

taken into account as riding atoms, with C—H = 0.97 Å for secondary CH₂ groups and 0.96 Å for methyl groups with $U_{\text{iso}}(\text{H}) = 1.2 U_{\text{eq}}$ (for secondary CH₂ groups) and $U_{\text{iso}}(\text{H}) = 1.5 U_{\text{eq}}$ (for methyl groups). The positions of the other H atoms were refined freely. The structures were drawn by ORTEP-3 for Windows [15] and Mercury [16] programs.

CALCULATIONS

The structural and electronic properties of the captopril drug, CAPDIS and CAPZn were investigated. All of the calculations were conducted under density functional theory (DFT) using the generalized gradient approximation (GGA) of the exchange-correlation potential as proposed by Perdew and Wang (PW91) [17], Perdew, Burke, and Ernzerhof (PBE) [18] and Becke [19] and Perdew [20], as implemented within the Quantum-ESPRESSO package PWscf [21]. The core electrons were described through ultrasoft pseudopotentials considering the following valence configuration: S: 3s² 3p⁴; O: 2s² 2p⁴; N: 2s² 2p³; C: 2s² 2p² and H: 1s¹. The valence electrons were expanded in plane waves with a kinetic energy cut-off of 60 and 480 Ry for the charge density cut-off. A 4×4×4 k -point sampling was used for the optimization calculations, and for the density of states (DOS) analyses an 8×8×8 k -point sampling was used. The k -point grid used for the optimization processes is able to reproduce electronic energies with an error lower than 10⁻³ Ry in comparison with larger k -point samplings.

RESULTS AND DISCUSSION

The crystal structure of captopril disulphide has recently been reported in the literature [22] and Fig. 1 displays the crystal structure of captopril disulphide. This compound is a dimer of the captopril drug. Captopril is highly susceptible to oxidation caused by high temperatures and humidity [6, 20]; thus, it is believed that the aqueous medium and the relatively high temperature used in the hydrothermal synthesis favoured the formation of captopril disulphide. The Zn²⁺ ion used in the synthesis acts as a catalyst for this reaction. This can be confirmed by performing the same synthetic route in the absence of the Zn²⁺ ion and by observing that captopril disulphide was not formed.

DFT under periodic boundary condition calculations for captopril and captopril disulphide was performed, and the results indicate that the cell parameters and geometry optimizations are in good agreement with the experimental data. For both compounds, the calculated cell parameters are overestimated, as observed in Table 1.

In captopril, the calculations show greater deviations in comparison with the experimental data [24]; the differences between the theoretical and experimental values are 0.469, 0.828, and 0.191 Å for *a*, *b*, and *c* parameters, respectively, presenting a maximum error of 5 %. These differences are smaller for captopril disulphide, which presents values of 0.199, 0.139, and 0.262 Å for *a*, *b*, and *c* parameters, respectively. Table 2 displays the selected geometrical parameters (experimental and theoretical) for both compounds. Comparing the geometrical parameters, it is observed that for captopril, the theoretical parameters present small average deviations (less than 2 %) for both types of calculations, relaxing only the atomic positions (relaxation calculations) and relaxing the atomic positions as well as the cell parameters (VC-relaxation calculations). The largest bond distance deviation was

Fig. 1. Crystal structure of captopril disulphide showing the atom numbering scheme. Anisotropic displacement ellipsoids are drawn at the 50 % probability level, and H atoms are shown as small spheres of arbitrary radii

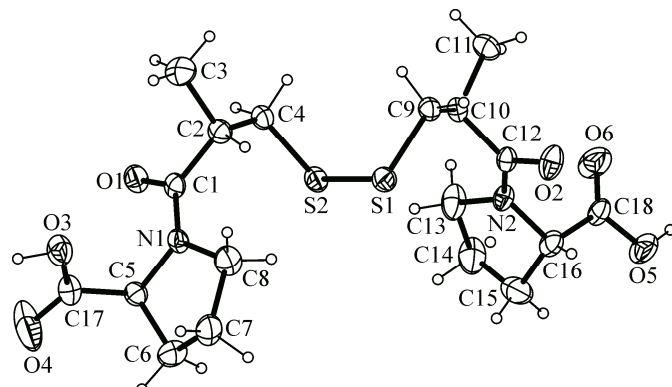


Table 1

Experimental and theoretical cell parameters for captopril [24], CAPZn [9], and CAPDIS [22]

Compound	<i>a</i> , Å	<i>b</i> , Å	<i>c</i> , Å	α , deg.	β , deg.	γ , deg.
Theoretical						
Captopril	9.280	18.812	7.028	90.00	90.00	90.00
CAPDIS	6.9636	11.2649	14.7973	90.00	91.8109	90.00
CAPZn	9.8250	9.8250	12.3999	90.00	90.00	90.00
Experimental						
Captopril	8.811(1)	17.984(2)	6.837(1)	90.00	90.00	90.00
CAPDIS	6.7642(3)	11.1262(6)	14.5062(8)	90.00	92.369(4)	90.00
CAPZn	9.6299	9.6299	12.1381	90.00	90.00	90.00

observed for C—O of the carboxylate group (5.5 %), and the largest deviation was for the S—C—C bond angle (2.3 %). Similar results were observed for the CAPDIS theoretical parameters, of which the average of the geometrical parameters is approximately 0.6 % for bond distances and 1.5 % for bond angles. The largest bond distance deviation was also observed for C—O of the carboxylate groups (approximately 5 %) and for the O—C—C bond angles (approximately 1 %). These structural results show that the theoretical protocols of the calculations can satisfactorily describe the bulk properties.

The crystal packing of captopril disulphide is stabilized by intramolecular and intermolecular hydrogen bonds. Non-classical intramolecular hydrogen bonds (C—H···O and C—H···S) can be observed in CAPDIS. An extensive network of intermolecular hydrogen bonds connects the captopril disulphide molecules into a supramolecular framework. It is convenient to consider individual substructures generated by different molecules of this compound in the asymmetric unit through intermolecular hydrogen bonds. The combination of those substructures builds a three-dimensional framework. Intermolecular O3—H3···O1 and O5—H5···O2 hydrogen bonds form zigzag chains (1D) along the *b* axis. These chains are linked to each other, giving rise to rings parallel to the (011) direction. In terms of graph-set notation, [25] these motifs can be represented as $N_1 = C(7)R_4^4(42)$. The three-dimensional design of the structure is observed through the C5—H5A···O4 weak hydrogen bonds and the graph-set notation for this net is $N_2 = C(7)$.

A comparison of the observed conformation of captopril disulphide with the commercial form conformation of captopril was also performed [24]. The main dihedral angles observed in captopril are 71.1(6) $^\circ$ (C3—C2—C1—S1), -17.0(6) $^\circ$ (N1—C8—C9—O3), 173.3(7) $^\circ$ (C8—N1—C4—C2) and -26.9(7) $^\circ$ (N1—C5—C6—C7). The equivalent angles in captopril disulphide are 174.4(3) $^\circ$ (S2—C1—C2—C3) and 172.4(3) $^\circ$ (S1—C10—C11—C12), -15.2(5) $^\circ$ (N1—C8—C9—O3) and -2.2(6) $^\circ$ (N2—C17—C18—O6), -180.0(3) $^\circ$ (C8—N1—C4—C2) and 174.7(3) $^\circ$ (C17—N2—C13—C11), 25.6(4) $^\circ$ (N1—C5—C6—C7) and 19.9(6) $^\circ$ (N2—C14—C15—C16). The major difference was found in the first dihedral angle, which is related to the sulphur atom. This is likely to be due to the formation of the S—S bond in captopril disulphide. Fig. 2 shows the superposition of the crystal structures of CAPDIS and captopril.

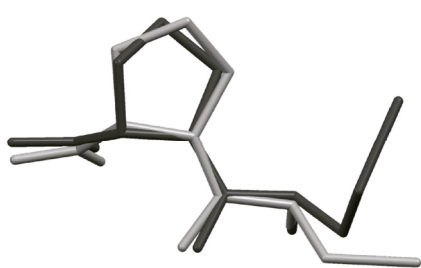


Fig. 2. Superposition of the crystal structures of CAPDIS and captopril. The hydrogen atoms are not displayed for clarity

Table 3 lists the main vibrational bands and assignments for captopril, CAPDIS, and CAPZn, and Fig. 3 displays the IR and Raman vibrational spectra of the same compounds. In the solid state, captopril molecules are organized in infinite chains linked

Table 2

Experimental and theoretical selected bond lengths (Å) and bond and torsion angles (deg.) of the captopril and CAPDIS compounds

Parameter	Exp.	Calc. (<i>n</i> -VC)			Calc. (VC)	
		PW91	BP86	PBE	PW91	
Bond distance						
Captopril						
C1—S1	1.827	1.829	1.834	1.829	1.832	
C4—O1	1.259	1.246	1.249	1.248	1.243	
C9—O2	1.299	1.371	1.371	1.369	1.371	
C9—O3	1.201	1.213	1.216	1.216	1.214	
CAPDIS						
S1—S2	2.037(1)	2.051	2.056	2.051	2.057	
S2—C4	1.809(4)	1.826	1.830	1.827	1.828	
C9—S1	1.814(3)	1.830	1.835	1.831	1.831	
C1—O1	1.246(4)	1.263	1.266	1.264	1.263	
C12—O2	1.241(4)	1.259	1.262	1.260	1.260	
C17—O3	1.276(5)	1.330	1.333	1.332	1.331	
C17—O4	1.195(5)	1.229	1.232	1.230	1.228	
C18—O6	1.169(5)	1.223	1.225	1.224	1.221	
C18—O5	1.296(5)	1.336	1.339	1.338	1.340	
Bond angle						
Captopril						
O2—C9—O3	121.88	119.47	119.47	119.72	119.79	
N1—C8—C9	110.61	110.99	111.70	111.85	111.82	
C7—C8—C9	111.95	112.77	112.54	112.55	111.99	
N1—C4—O1	119.34	118.94	119.08	118.92	119.42	
C2—C4—O1	121.60	120.53	120.19	120.27	120.81	
S1—C1—C2	112.13	114.30	114.55	114.93	114.72	
CAPDIS						
C4—S2—S1	103.7(1)	103.92	103.92	103.94	104.74	
C9—S1—S2	102.9(1)	103.47	103.45	103.44	104.04	
C2—C4—S2	115.6(3)	115.39	115.34	115.44	115.78	
C10—C9—S1	114.5(2)	114.13	113.99	114.20	114.77	
O5—C18—O6	125.6(5)	124.72	124.69	124.71	124.67	
O5—C18—C16	110.8(4)	111.86	111.95	111.87	111.88	
O6—C18—C16	123.5(4)	123.40	123.34	123.40	123.43	
O2—C12—N2	120.4(3)	120.89	120.88	120.89	121.05	
O2—C12—C10	119.8(3)	120.96	120.90	120.96	121.06	
O4—C17—O3	122.2(4)	123.58	123.60	123.60	123.54	
O4—C17—C5	120.0(4)	120.08	120.04	120.12	120.25	
O3—C17—C5	117.6(4)	116.31	116.32	116.25	116.17	
O1—C1—N1	120.1(3)	119.59	119.66	119.56	120.17	
O1—C1—C2	120.5(3)	121.76	121.53	121.75	121.50	
Torsion angle						
Captopril						
C3—C2—C1—S1	-170.5	179.37	177.08	176.93	179.51	
C4—C2—C1—S1	71.14	61.73	57.78	57.61	61.30	
CAPDIS						
C9—S1—S2—C4	-74.25	-75.40	-75.83	-74.76	-77.67	
S1—S2—C4—C2	-72.58	-71.09	-70.51	-71.53	-71.84	
S2—S1—C9—C10	-61.07	-58.89	-58.69	-59.16	-59.60	

Table 3

Principal IR and Raman bands (cm⁻¹) for captopril, CAPDIS, and CAPZn [9] compounds

Captopril		CAPDIS		CAPZn		Assignment ^a
IR ^b	Raman ^b	IR	Raman	IR	Raman	
2980m	2984s	2980w	2996s	2977m	2979vs	v(CH), v _a (CH ₃)
2936vw	2932s	—	2925vs	—	2921vs	v _a (CH ₂)
2878w	2880m	2887vw	2882s	2871w	2873s	v _s (CH ₂), v _s (CH ₃)
2566s	2568vs	—	—	—	—	v(SH)
1746s	1748m	1746m	1742w	—	—	v(CO)
—	—	—	—	1632vs	1631m	v _a (COO)
1602s	1586w	1602vs	1600w	1589s	1592w	v(CO) _{amide}
1473s	1474m	1474m	1476m	1469m	1469m	Δ _s (CH ₂)
—	—	—	—	1344vw	1346vw	v _s (COO)
1202m	1204vw	1186m	1183w	1201w	—	Δ(CH)
881m	—	886vw	884vw	—	—	Δ(OH _{out of plane})
676m	678vw	—	670vw	669w	671vw	v(CS)
—	—	—	512s	—	—	v(SS)
—	—	—	—	—	341w	v(ZnS)

^a Tentative assignment according to [23, 26, 28, 31]. v = stretching, a = antisymmetric, s = symmetric; Δ = deformation.

^b s = strong; m = medium; w = weak; v = very.

by hydrogen bonds involving carboxylic OH of one molecule and CO carbonyl of another molecule [26]. Due to the v(O—H···O) system, the IR spectrum of the free ligand exhibits a broad band in the range of 3000 to 2500 cm⁻¹, with satellites due to v(C—H) vibrations. The IR spectrum of the free captopril ligand shows one band with a strong intensity at 2566 cm⁻¹ (v(SH)), which is strong in the Raman spectrum. This band is not present in the spectra of CAPZn, suggesting deprotonation and coordination of the thiol group to the zinc ion. Furthermore, a band at 341 cm⁻¹ in the Raman spectrum of CAPZn has been assigned to v(Zn—S). The IR and Raman vibrational spectra of captopril also show a strong band at 1746 cm⁻¹ and 1748 cm⁻¹, respectively, due to the stretching mode [v(CO)]. This band disappeared in both spectra of the CAPZn complex, indicating the deprotonation of the carboxylic group and subsequent coordination. Two new bands were observed in the CAPZn spectra and

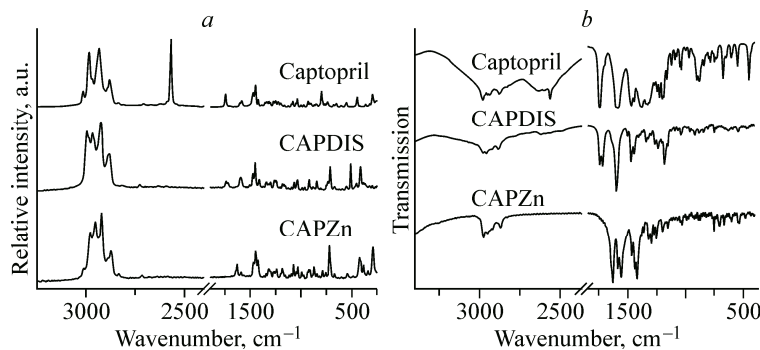


Fig. 3. Raman and (a) IR spectra of captopril, CAPDIS, and CAPZn [9] (b)

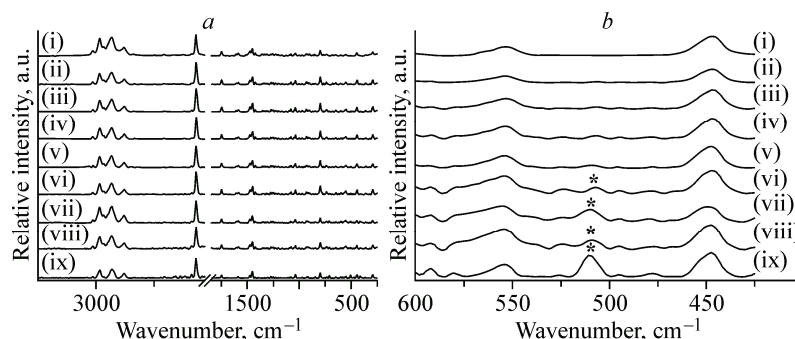


Fig. 4. Time-dependent Raman spectra of captopril (a), in the range of 600 to 425 cm^{-1} for: (i) 0 h; (ii) 1 week; (iii) 3 weeks; (iv) 4 weeks; (v) 5 weeks; (vi) 6 weeks; (vii) 9 weeks; (viii) 14 weeks and (ix) 35 weeks (b). The * represents the $v(\text{SS})$ mode

are attributed to $v_a(\text{COO})$ (1632 cm^{-1} in the IR spectrum and 1631 cm^{-1} in the Raman spectrum) and $v_s(\text{COO})$ (1344 cm^{-1} in the IR spectrum and 1346 cm^{-1} in the Raman spectrum). The difference (Δ) between the frequencies of these modes can be used to determine the coordination mode of the ligand to the metal site [27]. This information is related to the Δ values determined for the metal complex and ionic compounds. The frequency differences (Δ) determined from the IR spectra are 288 cm^{-1} for CAPZn and 145 cm^{-1} for sodium salt [28]. These values suggest that the coordination mode of the captopril drug to the metal site is monodentate in CAPZn, which is in agreement with the X-ray diffraction data [9]. The vibrational spectra (IR and Raman) of the captopril disulphide compound show vibrational modes of the main functional groups of the captopril molecule, such as the stretching modes of CO (1746 and 1742 cm^{-1} in IR and Raman spectra respectively), CO_{amide} (1602 and 1600 cm^{-1} in IR and Raman spectra, respectively), and CS (670 cm^{-1} in the Raman spectrum) bonds. The disappearance of the band at 2566 cm^{-1} ($v(\text{SH})$) in the IR and Raman spectra of CAPDIS is consistent with the formation of the S—S bond in CAPDIS. The Raman spectrum of CAPDIS shows a strong band centred at 512 cm^{-1} , which can be attributed to the S—S stretching mode [23].

A study of the stability of the captopril compound was conducted. The Raman spectra of captopril were performed during 35 weeks with humidity and air exposure to determine the stability of this drug with respect to the formation of captopril disulphide at room temperature. The time-dependent Raman spectra of captopril are shown in Fig. 4, a. There is a clear band at 2568 cm^{-1} assigned to the S—H stretching vibration mode of captopril. The intensity of this band decreased slightly with an increase in time. However, there was no significant modification for this mode over time, indicating that the captopril drug was still present. In addition, with an increase in time, a band at 512 cm^{-1} was observed for the captopril sample, possibly due to $v(\text{SS})$ of disulphide formation. The appearance of a weak band at 512 cm^{-1} was observed after 6 weeks of exposure of captopril in air (Fig. 4, b). The intensity of this band gradually increased over time. This band in particular was more intense after 35 weeks of exposure of the captopril drug, suggesting an increase in the quantity of captopril disulphide. The disulphide-related stretching vibrational band observed at 512 cm^{-1} in the Raman spectrum of the captopril sample indicates the unstable nature of captopril over time.

The unit cell crystallographic X-ray atomic coordinates of captopril, CAPDIS, and CAPZn were used as the initial point for DFT calculations in the solid state. For CAPZn, only the total densities of states (DOS) are presented. The total electronic energy was found in relaxation and VC-relaxation calculations for all compounds. The reaction used in the electronic energy variation (ΔE^{ele}) was the dimerization of captopril, forming captopril disulphide and H_2 . In all calculations, the CAPDIS compound is more stable than the captopril compound. In the relaxation calculations, ΔE^{ele} is -33.3 , -30.3 , and $-35.0\text{ kcal}\cdot\text{mol}^{-1}$ for PW91, PBE, and BP86 respectively, and $-28.5\text{ kcal}\cdot\text{mol}^{-1}$ for VC-relaxation under the PW91 exchange-correlation functional. These results corroborate the Raman spectroscopy evidence for the formation of CAPDIS from the dimerization process of captopril.

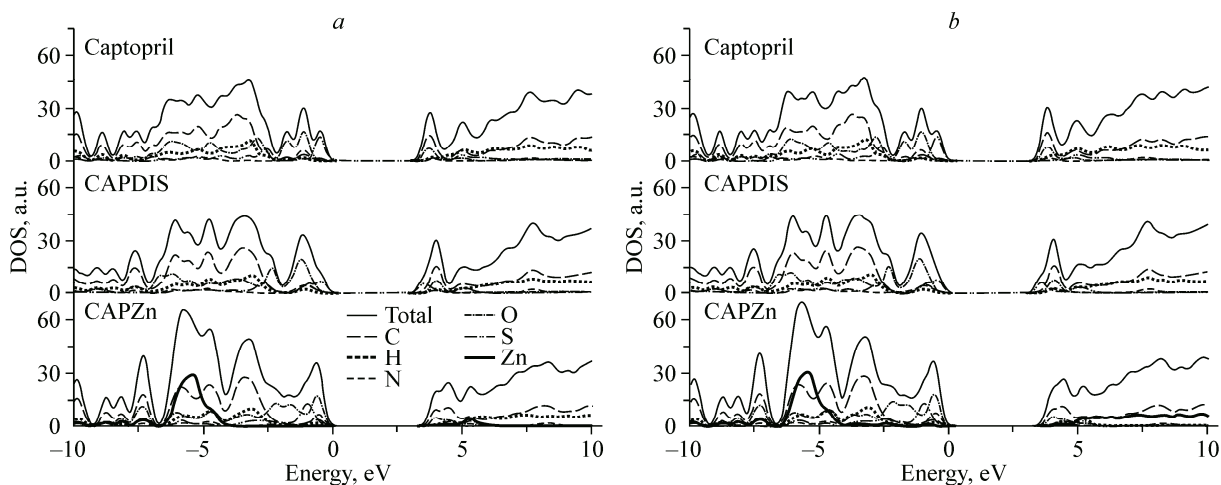


Fig. 5. The relaxation and (a) vc-relaxation total and partial densities of states for captopril, CAPDIS, and CAPZn (b)

The results for DOS, as well as the projected density of states (PDOS) for each atom, are very similar for the relaxation and VC-relaxation calculations, as observed in Fig. 5. The Fermi level shifted to 0 eV on the scale, corresponding to the valence band edge. For the captopril drug, the calculated energy gap is 3.1 and 3.2 eV for the relaxation and VC-relaxation calculations, respectively, and similar results were observed for CAPDIS (3.0 eV for relaxation and 3.2 eV for VC-relaxation). The CAPZn compound presented the largest values for the energy gap (3.4 in both calculations), but all of them can be classified as small band gap materials.

Comparing the total DOS for the captopril and CAPDIS compounds (Fig. 5), it can be observed that the main contribution to the valence band in captopril comes from the sulfur $3p$ orbital, and in CAPDIS, this contribution is mainly made by oxygen $2p$ and a minor contribution from the sulfur $3p$ orbital. However, in the conduction band, the major contributions came from the carbon and oxygen $2p$ orbitals for captopril and from the same atoms with a small contribution from the sulfur $3p$ orbital in CAPDIS. These results indicate that the sulfur atom is more available for coordination with the zinc atom of ACE in captopril drugs than in CAPDIS, which is in agreement with the experimental data that show greater biological activity of captopril in relation to CAPDIS molecules [6]. For the CAPZn complex, the greatest contribution comes from the oxygen, nitrogen, and carbon $2p$ orbitals, and in the conduction band, the major contributions came from the carbon and oxygen $2p$ orbitals.

The crystal structure of the CAPZn complex has recently been described in the literature [9]. The coordination sphere of the Zn^{2+} ion in the crystal is somewhat different than that suggested *in vivo* [8]. The refinement data demonstrate that a three-dimensional coordination polymer formed, and the Zn^{2+} ion also coordinates to the captopril carboxylate groups. An analysis of the connectivity net by the TOPOS program package [29] shows that the net associated with the structure consists of a 10-connected uninodal system and can be described with the point symbol $(3^{12}4^{18}5^{14}6)$ for Zn as vertices. The percentage of the unit cell volume occupancy is 69.3 %, providing 30.7 % of the free volume (346 \AA^3) [30]. The structural organization of the net suggests the presence of channels with small cavities in the structure, but the apparent pore volume and free space of the channels are filled by methyl groups of the ligand and the disordered pyrrolidine ring (Fig. 6).

CONCLUSIONS

Crystallographic data indicate that the captopril disulphide compound has been obtained under hydrothermal conditions from captopril. The structure determination reveals that this compound is a dimer of the captopril drug. The aqueous medium and a relatively high temperature used in the synthesis favoured the formation of captopril disulphide. The Zn^{2+} ion used in the synthesis acts as a catalyst for this reaction.

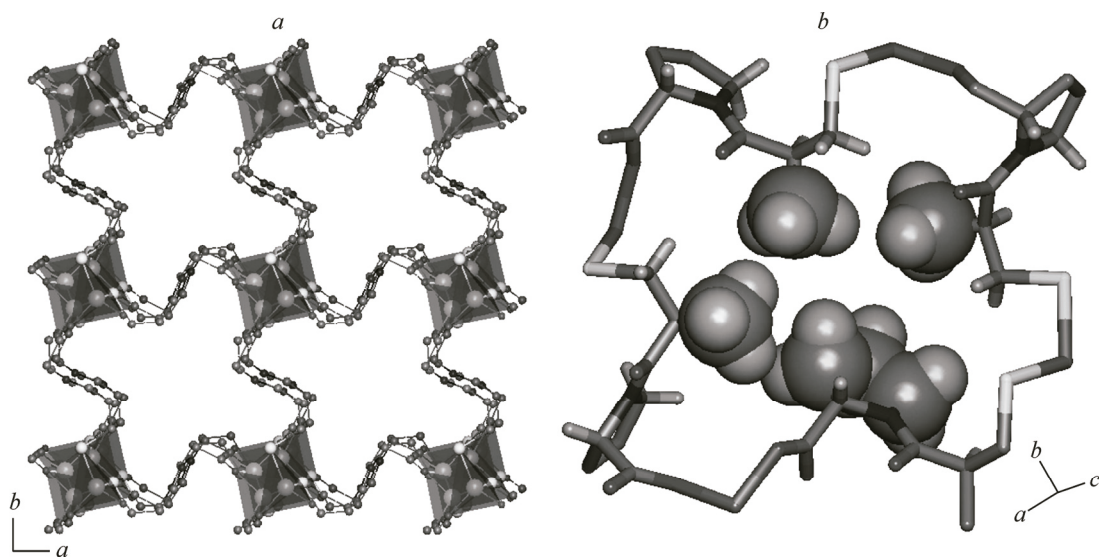


Fig. 6. Representation of the 3D net for CAPZn in the *ab* plane. Some atoms were omitted (*a*). Representation of methyl groups and the pyrrolidine ring in cavities of the channels (*b*). The figure was created by the TOPOS program package [29]

The Raman spectrum of CAPDIS shows a strong band at 512 cm^{-1} , which can be attributed to $\nu(\text{SS})$. This fact is consistent with the formation of the S—S bond. The disulphide-related stretching vibrational band observed at 512 cm^{-1} in the Raman spectrum of the captopril sample indicates the unstable nature of captopril over time. The variation of the electronic energy of captopril and CAPDIS in the solid state suggests an exothermic conversion of approximately $30\text{ kcal}\cdot\text{mol}^{-1}$ between them. The DOS results indicate that the sulfur atom is more available for coordination with the ACE zinc atom in captopril drugs than in CAPDIS, which is in agreement with the experimental data that show greater biological activity of captopril in relation to CAPDIS molecules.

An analysis of the CAPZn connectivity net by the TOPOS program package [29] shows that the net associated with the structure consists of a 10-connected uninodal system with tetrahedral Zn atoms and can be described with the point symbol $(3^{12}4^{18}5^{14}6)$ for Zn vertices.

The authors are thankful to the Brazilian Agencies CAPES, FAPEMIG, and CNPq for the financial support and LabCri (Universidade Federal de Minas Gerais) for X-ray facilities.

REFERENCES

1. Mahmoud W.M.M., Kummerer K. // Chemosphere. – 2012. – **88**. – P. 1170 – 1177.
2. Andrade J.P., Nobre F., Tavares A. et al. // Arq. Bras. Cardiol. – 2010. – **95**. – P. 1 – 51.
3. Kapungu G.P., Rukweza G., Tran T. et al. // J. Phys. Chem. A. – 2013. – **117**. – P. 2704 – 2717.
4. Mukherjee R., McCaddon A., Smith C.A. et al. // Inorg. Chem. – 2009. – **48**. – P. 9526 – 9534.
5. Wang J.K., Gao L., Liu Y. // J. Chem. Eng. Data. – 2010. – **55**. – P. 966 – 967.
6. Souza J.A.L., Albuquerque M.M., Junior S.G. et al. // Vib. Spectrosc. – 2012. – **62**. – P. 35 – 41.
7. Timmins P., Jackson I.M., Wang Y.J. // Int. J. Pharm. – 1982. – **11**. – P. 329 – 336.
8. Natesh R., Schwager S.L., Evans H.R. et al. // Biochemistry. – 2004. – **43**. – P. 8718 – 8724.
9. Yao J., Mo Y.H., Chen J.M. et al. // Cryst. Growth Des. – 2014. – **14**. – P. 2599 – 2604.
10. Andujar-Sanchez M., Camara-Artigas A., Jara-Perez V. // Biophys. Chem. – 2004. – **111**. – P. 183 – 189.
11. Natesh R., Schwager S.L., Sturrock E.D. et al. // Nature. – 2003. – **421**. – P. 551 – 554.
12. CrysAlisPro, in, Agilent Technologies, 2011.
13. Blessing R.H. // Acta Crystallogr., Sect. A. – 1995. – **51**. – P. 33 – 38.
14. Sheldrick G.M. // Acta Crystallogr., Sect. A. – 2008. – **64**. – P. 112 – 122.
15. Farrugia L.J. // J. Appl. Crystallogr. – 1997. – **30**. – P. 565.
16. Macrae C.F., Edgington P.R., McCabe P. et al. // J. Appl. Crystallogr. – 2006. – **39**. – P. 453 – 457.

17. Perdew J.P., Wang Y. // Phys. Rev. B: Solid State. – 1992. – **45**. – P. 13244 – 13249.
18. Perdew J.P., Burke K., Ernzerhof M. // Phys. Rev. Lett. – 1996. – **77**. – P. 3865 – 3868.
19. Becke A.D. // Phys. Rev. A: At., Mol., Opt. Phys. – 1988. – **38**. – P. 3098 – 3100.
20. Perdew J.P. // Phys. Rev. B: Condens. Matter. – 1986. – **33**. – P. 8822 – 8824.
21. Giannozzi P., Baroni S., Bonini N. et al. // J. Phys.: Condens. Matter. – 2009. – **21**. – P. 395502 – 395521.
22. Bojarska J., Maniukiewicz W., Fruzinski A. et al. // Acta Crystallogr., Sect. C. – 2015. – **71**. – P. 199.
23. Li M.J., Lin S.Y. // Photochem. Photobiol. – 2005. – **81**. – P. 1404 – 1410.
24. Fujinaga M., James M.N.G. // Acta Crystallogr., Sect. B. – 1980. – **36**. – P. 3196 – 3199.
25. Etter M.C., MacDonald J.C., Bernstein J. // Acta Crystallogr., Sect. B. – 1990. – **46**. – P. 256 – 262.
26. Jankovics H., Pettinari C., Marchetti F. et al. // J. Inorg. Biochem. – 2003. – **97**. – P. 370 – 376.
27. Deacon G.B., Phillips R.J. // Coord. Chem. Rev. – 1980. – **33**. – P. 227 – 250.
28. Atzei D., Sadun C., Pandolfi L. // Spectrochim. Acta, Part A. – 2000. – **56**. – P. 531 – 540.
29. Blatov V.A., Shevchenko A.P., Serezhkin V.N. // J. Appl. Crystallogr. – 2000. – **33**. – P. 1193 – 1193.
30. Spek A.L. // J. Appl. Crystallogr. – 2003. – **36**. – P. 7 – 13.
31. Bukovec P., Milicev S., Bukovec N. et al. // Inorg. Chim. Acta. – 1987. – **137**. – P. 177 – 180.